DARK MATTER SEARCHES AT BOULBY MINE - TOWARDS 1 TONNE XENON AND DIRECTIONAL DETECTORS

Neil Spooner*

Department of Physics and Astronomy

University of Sheffield, Hounsfield Rd., Sheffield S3 7RH, UK

Representing the UKDM Collaboration

ABSTRACT

Presented here is a review of the WIMP Dark Matter search programme at the Boulby underground laboratory. The programme comprises experiments based on liquid xenon technology (ZEPLIN) and a development project aimed at using low pressure gas to track nuclear recoils thus yielding a directional signal as well as discrimination (DRIFT). Correlation of recoils with our motion through the Galactic WIMP halo could give a definitive signal for dark matter. The first xenon experiment, ZEPLIN I (3.1 kg), is currently operational. Preliminary analysis has resulted in a limit with minimum approaching 10^{-6} pb (WIMP-nucleon cross section). Second generation detectors using simultaneous detection of ionisation and scintillation, ZEPLIN II (30 kg) and III (6 kg), are currently under construction with expected sensitivity at $<10^{-7}$ pb. To reach below 10^{-9} pb a detector of mass 1-10 tonnes is required. We present here new work on the sources and reduction of neutron background critical to the design of such a detector. A directional demonstrator experiment, DRIFT I, with 1 m^3 of negative ion gas is currently taking data and is described here. DRIFT II, with improved spatial resolution and target mass is currently under construction. First results on the use of Micromegas with CS$_2$ for future DRIFT detectors is presented.

1   Introduction

Evidence that the Universe contains cold dark matter has continued to strengthen in recent years. Precision measurements of the Doppler shift peaks in the cosmic microwave background measured by WMAP and continued observation of supernovae in distant galaxies strongly indicate that the Universe is well described by a ΛCDM model with cold dark matter accounting for around 23% of the mass-energy. On galactic scales, observation of rotation curves and gravitational lensing studies continue to require that galaxies contain up to 90% non-luminous matter. Meanwhile, particle physics provides a well motivated candidate particle, the weakly interacting neutralino of the supersymmetric family of models. Predictions and constraints imply a mass for such particles in the range around 50 GeV/c^2 - 1000 GeV/c^2, well matched to cosmology predictions for CDM but also accessible to direct searches using elastic scattering of atomic nuclei. Thus although the nature of the dark matter, responsible as it is for the structure of our Universe, is one of the biggest questions in science, there is a well motivated and feasible route to a solution - the construction of experiments sensitive enough to record the rare nuclear recoils induced by dark matter particles as they interact here on Earth, hence to prove that WIMPs (Weakly Interacting Massive Particles) are the dark matter.

The UK Dark Matter Collaboration (University of Sheffield, University of Edinburgh, ICL and RAL) currently run such a programme of dark matter experiments in collaboration with several groups from Europe and the US (UCLA, Texas A&M, ITEP, Coimbra, Occidental College and Temple University). The base for this activity is the newly upgraded Boulby Underground Laboratory (see Figure 1) which, at a vertical depth of 2800 m.w.e. (muon flux 4.1×10^{-8} cm^{-2} s^{-1}) and with 1500 m^2 of new environmentally controlled laboratory space, provides excellent facilities for dark matter and other experiments requiring suppression of cosmic-ray muons and associated neutrons.[1–3] The Boulby programme produced the first competitive limits with NaI targets in 1996,[4] improving these limits further through construction of the NAIAD detector using unencapsulated NaI.[5] The NaI technology, which uses pulse shape discrimination as a means of statistically suppressing electron recoil background, provided a firm base for first generation dark matter searches, including the development of analysis techniques. However, the relatively poor discrimination power of this technology, restricted to energies

above 4 keV (visible energy), and the difficulty of extracting radioactive impurities, restricts its sensitivity reach to the region around 10^{-5} pb. The ZEPLIN programme at Boulby, using liquid xenon technology, addresses both these issues. The DRIFT programme, using low pressure gas, also addresses these issues but with the additional merit of potential capability of measuring the direction of WIMP induced recoils, and providing a variety of targets of both low and high A in a radical new technology complementary to xenon.
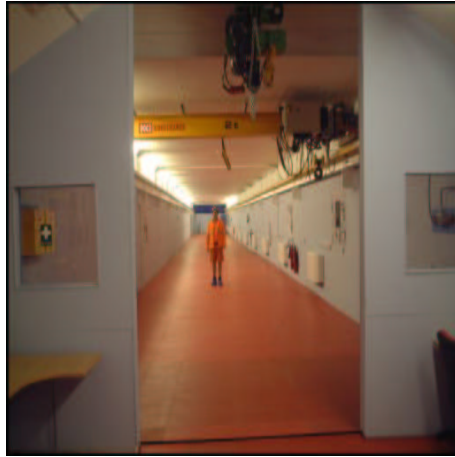

Figure 1: The main underground hall at Boulby.

2   Liquid Xenon for Dark Matter Searches

As indicated above there are two key requirements for direct dark matter detection technology: (1) low intrinsic radioactive background from detector and surrounding components, principally this means U/Th and K contamination well below ppb and ppm levels respectively, and (2) good recoil discrimination, to allow rejection of remaining electron recoil background. Nuclear recoil discrimination in liquid xenon is feasible by measuring both the scintillation light and the ionisation produced during an interaction, either directly or through secondary recombination. Meanwhile, the chemical inertness and isotopic composition of liquid xenon provide intrinsically low radio-purity and routes, in principle, to further purification via distillation, centrifuging and chromatography. The heavy nuclei of xenon also has the advantage of providing a large spin-independent coupling.

The interaction processes in liquid xenon are illustrated in Figure 2. Energy is distributed between two processes. Firstly, the production and decay of excited Xe_2^* states. These decay, through singlet and triplet states, with time constants 3 ns and 27 ns respectively, emitting 175 nm photons. The dE/dx of the recoil determines the proportion of energy channelled into these two decay modes, such that the ratio of singlet to triplet is an order of magnitude greater for nuclear recoils over electron recoils. The nuclear recoils thus produce a scintillation pulse through the excited dimer which is significantly faster than for electron recoils. Secondly, the production of ionisation via ionised state Xe_2^+. This ionised dimer can recombine with the liberated free electrons giving Xe_2^* states which decay through the excited dimer channel above. This recombination can be suppressed by the application of an electric field, such that the ionisation yield from this process can be directly measured. If the recombination is allowed to occur then the dE/dx of the incident particle determines the recombination time. For nuclear recoils the recombination occurs within picoseconds of the interaction, for electron recoils the recombination time is of order 40 ns.
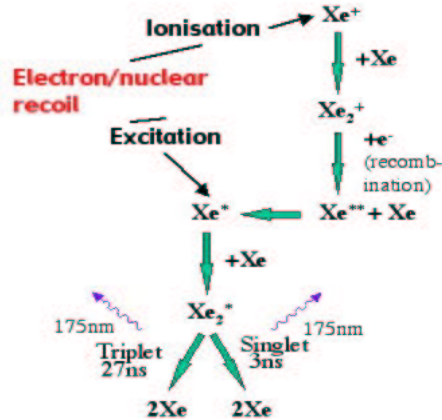

Figure 2: Interaction processes in liquid xenon.

These processes provide several means of obtaining recoil discrimination in liquid xenon. In a single phase (liquid only) detector, such as ZEPLIN I (see sec. 3.1), the nuclear recoil discrimination is performed through pulse shape analysis, determining the emission time constant of the scintillation light. This includes components from both direct excitation and recombination, the recombination

time during an electron recoil extending the scintillation time constant. For two-phase detectors, such as ZEPLIN II and III, the presence of an electric field allows the ionisation to be collected and measured directly or observed in the gas phase through electroluminescence. This is made possible by the ease with which electrons can be drifted through the liquid phase and extracted into the gas phase. The efficiency of the ionisation separation process depends on the initial linear ionisation density. The time-constant of the scintillation signal is affected by the charge collection, as it enhances the ionisation signal at the expense of the scintillation signal. The effect will be most pronounced for gamma-ray interactions where the ionisation track tends to be less dense and the electric field will be more effective at separating the free electrons from the ions. Once separated, the electrons will drift in the field until they reach the xenon liquid surface where they can be extracted into the gas phase. Once in the gas phase the electrons are drifted into a high field region where they produce a secondary scintillation, or electroluminescence, which is proportional to the amount of charge extracted.

3   The ZEPLIN Experiments

The ZEPLIN programme (Zoned Proportional scintillation in LIquid Noble gases) aims, thourgh a series of technology demonstrator experiments based on the liquid xenon properties described above, to develop a WIMP search detector capable of reaching the lowest predicted neutralino cross sections, around 10^{-10} pb. The following sections describe the demonstrator experiments, ZEPLIN I, II and III, themselves designed to push sensitivity towards 10^{-8} pb. Section 4 details work towards development of a very large xenon detector of mass 1-10 tonnes.

3.1   ZEPLIN I

The first detector of the ZEPLIN development series, ZEPLIN I, uses the simplest single phase concept in which recombination is allowed in-situ so that each event, nuclear or electron, produces one scintillation pulse. Discrimination is then based on pulse shape analysis of these pulses by techniques identical to that used in the NAIAD NaI-based technology, except that for xenon the pulse shapes are faster and the mean time constant ratio (electron over nuclear recoil) larger (see sec. 2).

   A diagramme of the detector, installed in Boulby in 2001 and currently run-

ning, is shown in Figure 3. The liquid xenon, a total fiducial mass of 3.1 kg, is viewed by 3 PMTs through silica windows. Between each PMT and the main volume is a turret structure containing liquid xenon optically decoupled from the other two PMTs so that light from interactions in these regions is only seen in the nearby PMT. This provides a means of discriminating against events due to x-rays produced by activity in the PMT windows and surroundings.
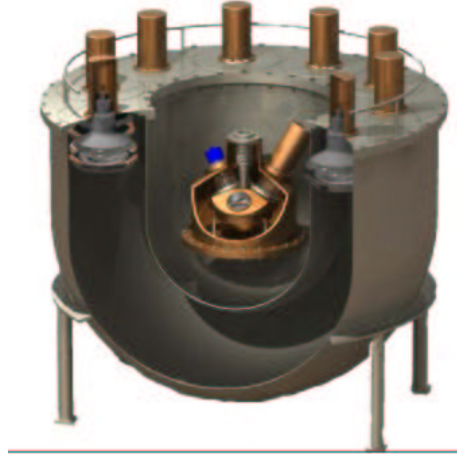

Figure 3: The ZEPLIN I detector.

The main detector vessel, fabricated from high purity copper, is enclosed in a vacuum jacket and supplied with cooling fluid from a Polycold chiller. High energy gammas from the down-pointing PMTs may produce Compton scatters in the target in the energy range of interest (10-200 keV). Hence a 1 tonne hemispherical active Compton veto is provided around the main vessel. This is constructed using PXE liquid scintillator viewed by 10 x 8 inch hemispherical PMTs. The efficiency is estimated from Monte Carlo simulations to be 80-90% below 100 keV. The output of the veto, placed in anticoincidence with the target, allows suppression of these Compton events. Xenon purity is a key influence on the operation of liquid xenon detectors, in particular of the scintillation light yield and electron transport. For ZEPLIN I purification is performed using a combination of Oxisorb filtration and fractionation of the Xe gas following pumping on the frozen Xe.

The detector PMTs are placed in a three-fold coincidence at a trigger threshold of 1 p.e. per tube. This results in a trigger threshold of 2 keV assuming a light collection of 1.5 p.e./keV. Signals from the PMTs are passed through an integrat-

ing buffer and digitised using an Acqiris cPCI-based data acquisition system with remote access from the site via optical cable. The dead-time during normal data runs is less that 0.1%.

Calibration of ZEPLIN I with sources is a vital part of the data analysis process, needed to define the pulse shape distributions for background electron recoil events and nuclear recoils and to ensure stable energy calibration. The detector is provided with an automatic gamma energy calibration process for this via a source dropping apparatus that places a ^{57}Co source between the target and veto once per day. This yields 122 keV gamma events in the target and 30 keV K-shell x-rays. This source, plus less frequent use of ^{60}Co, also provides a means of defining the gamma pulse shape constant distribution vs. energy. Events tagged by the Compton veto (principally high energy PMT gammas) can also be used for time constant calibration. Separate calibration with a ^{252}Cf neutron source provides a means of determining the, shorter, time constant distribution for nuclear recoils. Example calibration data are shown in Figure 4. It is the difference in time constant distributions between recoils and electron background that provides ZEPLIN I with discrimination capability. Neutron and gamma source calibrations performed on the surface have shown nuclear recoil time constants typically 55-60% of a typical electron time constant (see Figure 4).
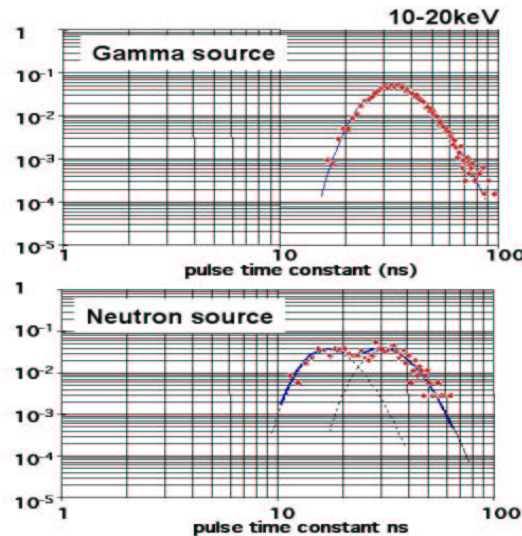

Figure 4: Example ZEPLIN I calibration data.

The response of the detector to interactions depends significantly on the posi-

tion of the event within the xenon due to variation in the light collection efficiency, varying from 4% near the xenon delivery line to around 18% at the bottom of the target equidistant from the PMTs. A light collection Monte Carlo model of the complete xenon volume, including turret areas, is used to determine this response function in detail. Figure 5 shows example light collection distributions. The response function is used to help define a fiducial cut parameter S_3 based on the relative size of pulse in the three tubes for each event. Events near the centre of the detector are expected to produce pulses of near equal amplitude, $S_3 = 0$, and are passed by the cut. An event in or near a turret region will result in asymmetric pulses with corresponding $S_3 > 0$, the extreme case being $S_3 = 0.81$ if only one PMT records light. A suitable, lower, choice of S_3 allows 90% of turret events to be rejected leaving an effective 100% active mass of 3.1 kg.
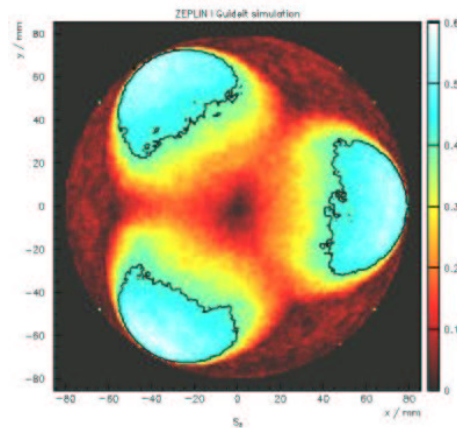

Figure 5: Example light collection simulation data.

It is important with xenon detectors to assess the possibility of ^{85}Kr contamination. A limit on this level can be achieved from examination of the raw background spectrum, following application of S_3 cuts. Early runs used standard research grade xenon (typically 5 ppm Kr) for which a level of 10^{-17} atoms-per-atom was measured in this way, assuming Kr as the main background source. More recently low Kr (40 ppb) xenon has been used. This displayed a factor 3 reduction in background but additionally also appeared to result in an increase in light yield up to 2.5 p.e./keV. The latter may be explained by the purification process which may remove other contaminants from the xenon such as CO_2.

Examination of the rising left-hand edge of the time constant distribution for data in each energy bin allows a 90% c.l. limit to be placed on the number of nuclear recoil events (with their faster time constants) in that energy bin. This is converted into a WIMP-nucleon cross section limit and the results for each energy bin combined to produce an overall limit. Figure 6 shows a preliminary limit extracted from 230 kg-days of data analysed by this method. It can be seen that the resulting limit is wholly below the signal region favoured by DAMA[6] and produces the lowest current limit in the intermediate mass range of 30-70 GeV. Results from CDMS[7] and Edelweiss[8] also can not be reconciled with DAMA. Further analysis is currently underway of data taken with the reduced Kr xenon which is expected to produce further reduction in the limit.
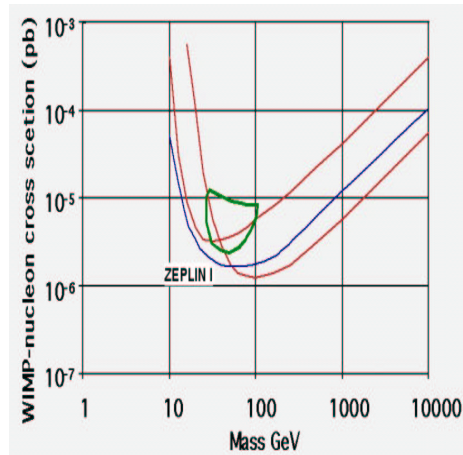

Figure 6: Summary of ZEPLIN I WIMP limits. Also shown are limits from CDMS (upper curve), Edelweiss (right curve) and the allowed region of DAMA.

3.2 ZEPLIN II

The Boulby collaboration is currently constructing the next generation of ZEPLIN demonstrator detectors ZEPLIN II and III. These both use two phase xenon (a gas region above the liquid xenon is used). The main discrimination power comes then from the relative area of the scintillation signal (primary pulse) compared with an ionisation (secondary luminescence) signal, the latter generated in the gas by avalanche following extraction using an electric field in the liquid. Both signals

are seen as photons, with a time delay between them, the primary scintillation signal occurring first. For a given primary amplitude a gamma-ray will produce a much larger secondary than a nuclear recoil (see sec. 2). A simple primary to secondary amplitude ratio provides a powerful discrimination parameter, first demonstrated by the UCLA group in a low-field operation where there was no secondary signal from nuclear recoils.[9,10]

The ZEPLIN II detector is a scaled up version of the UCLA prototype, measuring both scintillation and ionisation but with an electric field in the liquid sufficient only to extract the charge. Figure 7 shows a schematic of the detector. A target mass of 30 kg is viewed by an array of 7 PMTs situated above the liquid and above the gas. A wire plane in the gas phase defines a high field region in which the avalanche is created and electroluminescence photons produced. The PMTs are positioned to detect the scintillation from both the primary and the secondary electroluminescence. A compton veto will also be provided around the detector for the same reasons as was required by ZEPLIN I (see sec. 3.1).
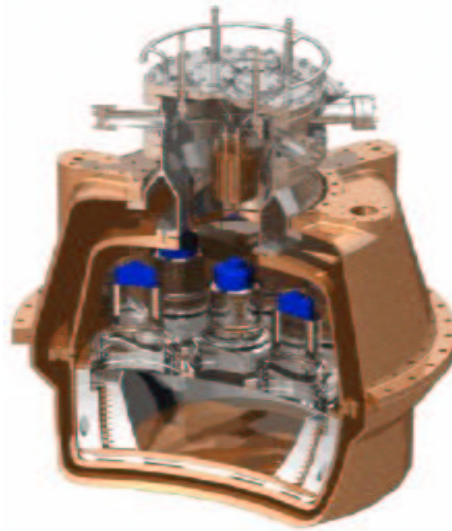

Figure 7: Drawing of the ZEPLIN II detector.

Commissioning of ZEPLIN II is currently underway with installation anticipated at Boulby in early 2004. The predicted sensitivity of ZEPLIN II is expected to be up to two orders of magnitude better than ZEPLIN I.

3.3 ZEPLIN III

The ZEPLIN III experiment represents an attempt to run in two phase mode but with much higher electric field in the liquid region (typically 8 kV/cm). The advantage of this is the prospect of recording a small ionisation signal from the nuclear recoils, as well as from the electron background events, and of improving the energy threshold. Figure 8 shows a schematic of ZEPLIN III. The active target comprises a cylinder of liquid xenon of 3.5 cm depth and radius 20 cm. Above this is the gas region with avalanche mesh and a reflective plate that directs light down towards an array of 31 PMTs submerged within further liquid xenon below the fiducial volume. As with ZEPLIN II the PMTs record both the primary and secondary signals. The position of the PMTs within the liquid improves light collection and hence reduces the energy threshold compared to that predicted for ZEPLIN II. With this design the fiducial volume is restricted to 6 kg, largely by the difficulty of supplying high voltage into the array. Despite this the sensitivity anticipated is close to that of ZEPLIN II. The detector is currently being assembled with installation anticipated at Boulby during 2004.
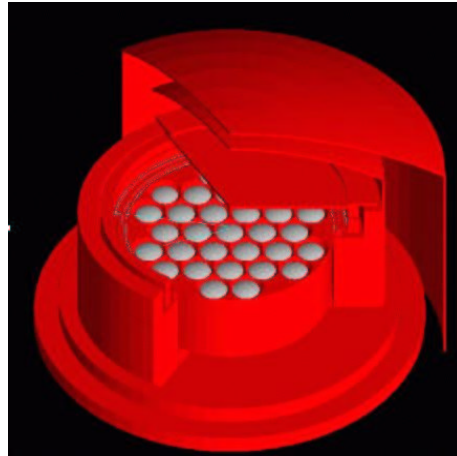

Figure 8: Drawing of the ZEPLIN III detector.

4 A Very Large Xenon Detector

The ZEPLIN programme described above can be viewed as a development sequence aimed at determining the optimum design for a large scale (1-10 tonne)

xenon detector capable of sensitivity below 10^{-9} pb in 1 year of operation. Such a large mass is required simply to achieve sufficient signal counts in a year (say 10 - 100 events). A pre-requisite for such a detector, given the likely limitations on intrinsic radio-purity of detector components, is also gamma discrimination at a level more than 10^5. This level of electron background rejection, probably with the addition of statistical reduction techniques, is actually already within reach using xenon and is expected to be demonstrated by the ZEPLIN programme. Scaling from 30 kg (ZEPLIN II design - success assumed) to 1000 kg via an array of say 4 of 250 kg modules probably does not present insurmountable obstacles. However, there remains a key critical path issue that needs addressing to demonstrate feasibility - the issue of neutron background. The rate of neutrons from U and Th contamination in detector and surrounding materials is typically 10^5-10^6 lower than that from gammas in the energy range of interest. Hence, assuming gamma discrimination at > 1 in 10^5 is achieved (necessary anyway to reach 10^{-10} pb), then detector neutrons may become a dominant intrinsic background which, furthermore, can not be actively discriminated against because they produce nuclear recoils indistinguishable from WIMP induced events. There remains also two further sources of neutron events, from fission in the rock and from high energy muons.

This section summarises new work aimed at assessing the significance of the three sources of neutron background in a large scale xenon detector, leading to definition of design criteria required to ensure neutrons are not a limiting factor to sensitivity. Further details can be found in.[11]

4.1 Neutrons from Rock

The objective here was to find the thickness of hydrocarbon shielding needed to suppress the neutron flux from rock to the required level. This was achieved in 4 stages: (1) simulation of neutron production in rock, (2) propagation through rock to the rock/cavern boundary, (3) propagation through Pb gamma shielding and hydrocarbon to the detector, and (4) generation of nuclear recoil events in the xenon target. Neutron production via spontaneous fission and (α,n) reactions in rock was carried out with a modified version of the SOURCES code assuming halite rock using typical contamination levels of 60 ppb of U and 300 ppb of Th in secular equilibrium. The neutron production rate was found to be about $1.05 \times$

10^{-7}cm^{-3} s^{-1}. The neutron energy spectra in NaCl obtained with SOURCES are similar for U and Th initiated neutrons. Uranium gives roughly twice as many neutrons as thorium.

Neutron propagation through the rock was simulated using the GEANT4 package.[12] Neutrons from the rock wall were produced in a slab of rock 1×1 m^2 area and 3 m depth and allowed to propagate isotropically into a much larger region (100×100m^2) and the total spectrum then re-scaled to the original 1×1 m^2. Parameters for the neutrons reaching the rock/cavern boundary were stored prior to propagation of the neutrons through lead and hydrocarbon shielding. Simulations were also run for a realistic cavern with a size of $30 \times 6.5 \times 4.5$ m^3 (see Figure 9). The neutron flux for this configuration at the rock/cavern boundary was found to be 4.25×10^{-6} cm^{-2} s^{-1} above 10 keV and 3.38×10^{-6} cm^{-2} s^{-1} above 100 keV. To check the effect of back-scattering, neutrons were also propagated through the cavern and counted each time they entered the cavern. In this case the calculated neutron flux was 1.51×10^{-5} cm^{-2} s^{-1} above 10 keV and 9.25×10^{-6} cm^{-2} s^{-1} above 100 keV.
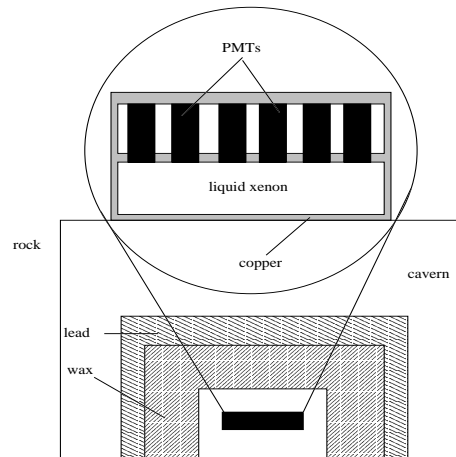
Figure 9: Sketch of the laboratory hall with a xenon detector and shielding inside.

Lead, of low radioactivity and typically 30 cm thickness (or equivalent) is required for gamma shielding. Hence, simulations were carried out with and without lead to investigate its influence on the neutron flux. Neutrons coming from the rock in a simple geometry (neutron production volume – $1 \times 1 \times 3$ m^3, neutron propagation volume – $100 \times 100 \times 3$ m^3) were propagated through the lead,

with account taken that neutrons can be scattered back from the lead into the rock and then to the lead again. Hydrocarbon of varying thicknesses was added after the lead. Figure 10a shows neutron spectra after 30 cm of lead and slabs of hydrocarbon of various thickness. Figure 10b shows similar spectra obtained without lead. We can conclude that using 35 g/cm^2 of hydrocarbon material together with 30 cm of lead or 50 g/cm^2 of hydrocarbon material without lead the neutron flux can be suppressed by about six orders of magnitude.
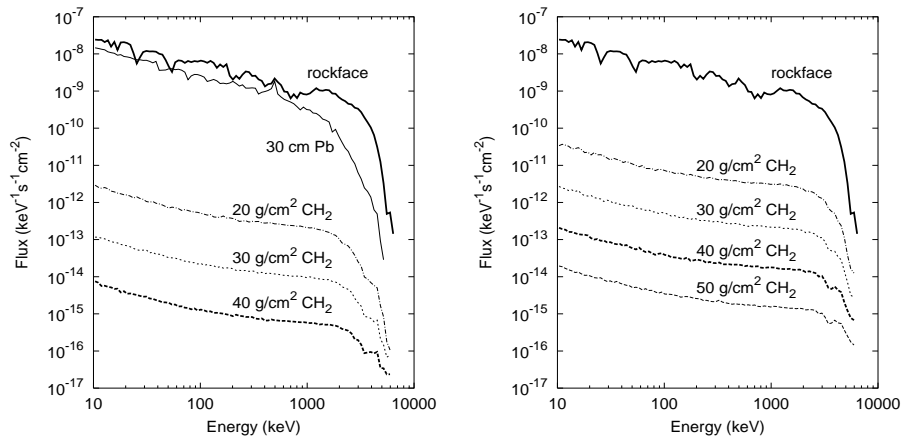

Figure 10: Neutron energy spectra from rock activity after lead (left graph only) and hydrocarbon shielding: (a) left graph– with 30 cm of lead between salt and hydrocarbon; (b) right graph– without lead. Neutrons were propagated using GEANT4. The initial neutron production spectrum was obtained with modified SOURCES. Thick solid curve – spectrum at the salt/cavern boundary; thin solid curve – spectrum after 30 cm of lead (left graph only); dash-dotted curve – spectrum after 20 g/cm^2 of hydrocarbon shielding behind lead (left) or without lead (right); dotted curve – spectrum after 30 g/cm^2 of hydrocarbon; thick dashed curve – spectrum after 40 g/cm^2 of hydrocarbon; thin dashed curve – spectrum after 50 g/cm^2 of hydrocarbon (right).

Simulations of the nuclear recoil energy spectrum in a large-scale xenon detector were carried out with GEANT4 using the model neutron spectrum, the laboratory geometry as above and a model 250 kg xenon detector comprising a cylinder with a diameter of 103 cm, height of 10 cm and density of 3 g/cm^3 surrounded by 35 g/cm^2 of hydrocarbon material and 30 cm of lead. The resulting

event rate in a 10-50 keV recoil energy range was found to be 0.86 events per year. We conclude that 35-40 g/cm^2 of hydrocarbon and 30 cm of lead are enough to suppress the neutron flux from rock activity down to an unobservable level.

4.2   Neutrons from Muons

Even at depth muons are a likely important source of neutrons. To investigate this the muon spectrum and angular distribution was simulated using the MUSUN Monte Carlo code[2] with normalisation using the measured muon flux at Boulby of $(4.09 \pm 0.15) \times 10^{-8}$ cm^{-2} s^{-1}. Simulations of the muon propagation and interactions, development of muon-induced cascades, neutron production, propagation and detection were performed with FLUKA.[13] For other sites at a similar depth the neutron flux can be scaled roughly as the muon flux. Variation of the muon energy spectrum with depth can be accounted for using the known dependence of neutron production on the mean muon energy and changes in the neutron flux due to rock composition can be estimated through the dependence of the neutron production on the mean atomic weight of the rock as $\propto A^{0.76}$.[2] Muons were sampled on the surface of a cube of rock (NaCl) $20 \times 20 \times 20$ m^3 inside of which was placed the laboratory of size $6 \times 6 \times 5$ m^3. The cavern contained shielding made of lead and hydrocarbon material. A cylindrical vessel (103 cm diameter, 10 cm height) made of stainless steel of thickness of 2 cm containing 250 kg of liquid xenon (density 3 g/cm^3) was placed inside the shield (as in sec. 4.1).

Figure 11 shows the effects of lead and hydrocarbon material on neutron production and absorption. Neutron spectra on the rock/cavern boundary and after the lead (lead/cavern boundary) are presented in Figure 11a. The large increase in the neutron spectrum after the lead is due to the efficiency of neutron production in lead. Hydrocarbon material suppresses this flux by a large factor at low energies (Figure 11b). This figure demonstrates the potential danger of placing lead shielding close to the detector and inside the hydrocarbon shielding. An active veto system may help to reject events associated with muons but not with 100% efficiency if placed around the main detector and the lead shielding. The neutron flux is suppressed by a factor of $10^2 - 10^4$ by 40 g/cm^2 of hydrocarbon shielding at energies 0.1-10 MeV, most important for low-energy nuclear recoil production in xenon. To achieve similar suppression with an active veto system would require an efficiency of 0.9999.
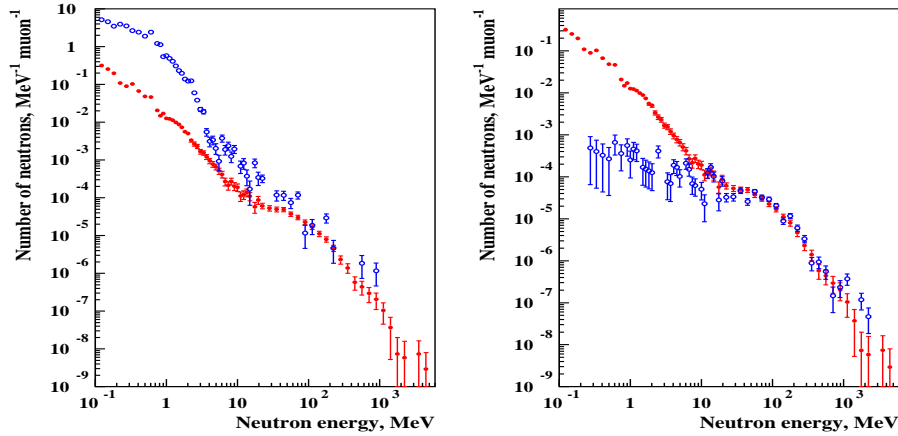
Figure 11: Energy spectra of muon-induced neutrons at various boundaries: (a) left – filled circles - neutrons at the salt/cavern boundary; open circles - neutrons after the lead shielding; (b) right – filled circles - neutrons at the salt/cavern boundary (same as on the left graph); open circles - neutrons after the lead and hydrocarbon shielding.

Figure 12 shows the energy spectrum of nuclear recoil events originating from muon-induced neutrons in the model detector. Events with multiple recoils were assigned an energy equal to the sum of the individual nuclear recoil energies, but excluding energy depositions due to processes not associated with neutron elastic scattering. About 20 million muons were simulated which yielded a total of 250 nuclear recoil events per year in the detector. This also includes events where nuclear recoils are in coincidence with any other form of energy deposition (electrons, photons, muons etc.). 25 events per year have nuclear recoils only without any other energy deposition. This is the number that determines the sensitivity of the detector to WIMPs since other events will be rejected as electron-like events. 11 events per year are single nuclear recoils. Finally 7.5 nuclear recoil events per year (without electron-like component) are expected to be within an energy range of interest for dark matter searches (10-50 keV recoil energy).

We also considered use of a hydrocarbon scintillator active veto situated between the xenon and lead shielding. To check the efficiency of such a veto only those events detected in anticoincidence between the main xenon detector and scintillator veto made of 40 g/cm^2 thick hydrocarbon were recorded. No events
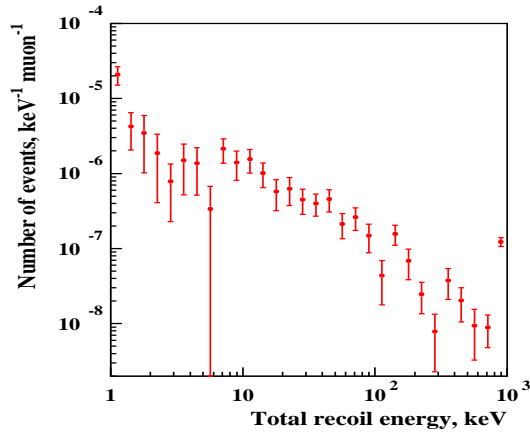
Figure 12: Recoil energy spectrum in a 250 kg liquid xenon detector from muon-induced neutrons. The energy of all recoils in any particular event was summed to give the energy of each event. The highest energy point plotted also includes all events above 1 MeV.

occurring in the target were detected in anticoincidence with a hydrocarbon scintillator.

4.3   Neutrons from Detector Components

Neutrons from detector components are likely to be the dominant source of background in any detector aimed to reach $<10^{-9}$ pb. It can come from the readout system, target, vessel walls and shielding. For all these components the actual contamination levels are not known precisely. However, for a large scale xenon detector with conventional readout the PMTs and their bases probably constitute the most serious limitation.

To investigate this two types of low background PMTs were used to simulate the PMT related neutron background: 2-inch ETL type 9266 PMTs, modelled as a cylinder of glass, metals and ceramics, and the new 2-inch Hamamatsu R8778 tube, modelled as a cylinder of quartz and metals. A cylindrical detector of 250 kg xenon, was viewed by either 217 ETL 9266 PMTs or 169 R8778 PMTs with hydrocarbon material placed between PMTs to reduce the neutron flux. The setup

included 1 cm thick copper walls around the liquid xenon and PMTs, a 1 cm thick copper support structure for the PMTs and an acrylic absorber between PMTs to suppress the neutron flux (see Figure 9). The ETL 9266 PMT has a borosilicate glass window opaque to VUV. Hence, it is assumed here that a low background wavelength shifter can be applied to the window. The contamination levels for the ETL 9266 PMT were taken from[14] and for the R8778 PMTs estimated from.[15]

The SOURCES code, modified appropriately, was used to obtain neutron spectra from the materials and the appropriate spectra propagated through the detector. If a neutron scattered two or more times then the energies of all recoils were added up to obtain the total event energy. It was assumed again that the detector had a step function energy threshold of 2 keV (visible) and we used a 2-10 keV energy range.

Results show that about 300 events per year are expected in the detector with ETL 9266 PMTs and 7.6 neutrons per year for the R8778 version. Several methods can be used to reduce these numbers. For instance 5 cm thick low background acrylic (Plexiglas) lightguides with wavelength shifter between PMTs and xenon can reduce the nuclear recoil rate from PMTs by a factor of 2 giving 3.6 events per year from the R8778 PMTs. Reducing the contamination levels of PMTs and making these PMTs of larger (5-inch) size will improve the sensitivity of future detectors. A level of 0.5 ppb U and Th in the PMTs results in 0.9 events per year while use of 5 inch PMTs reduces the rate to about 0.4 events per year, due to the consequent reduced mass. Although the level of impurities used in PMT dividers (in particular ceramics) reaches 100-1000 ppb of U and Th the mass involved is small and can be reduced using new chip resistors and film capacitors bringing the number of events from this source below the PMT contribution. Although the copper vessel is assumed to be heavy (total weight typically 350 kg), impurity levels are obtainable below 0.02 ppb. The nuclear recoil rate from this is found to be about 0.4 events per year.

Adding up the contributions it is concluded that of the order of 4-8 events per year in 250 kg of liquid xenon (10-50 keV recoil energy) is achievable, with reduction to 1 event per year through success with PMT developments. Similar or even larger reduction could be achieved with new readout designs, such as based on GEM[16] or MICROMEGAS[17] currently being studied for large dark matter detectors[18,19] (see sec. 5.4). These use materials, such as copper, Kapton and Teflon, all with very low levels of impurities, reducing the number of expected events to

less than 1 event per year. Another possibility is to estimate the background by independent techniques and subtract the estimated value from the measurements.

4.4 Sensitivity of a Large Scale Xenon Detector

Based on the neutron simulations above, and assuming that the expected gamma and alpha background discrimination factors are achievable, we can estimate the sensitivity of a large xenon detector. Results are summarised in Figure 13 for a 250 kg xenon detector running for a year, presented in conventional terms of limits on WIMP cross-section as a function of WIMP mass. An isothermal spherical halo with 0.3 GeV/cm^3 WIMP density and Maxwellian WIMP velocity distribution was assumed and the procedure described by Lewin and Smith[20] was followed.
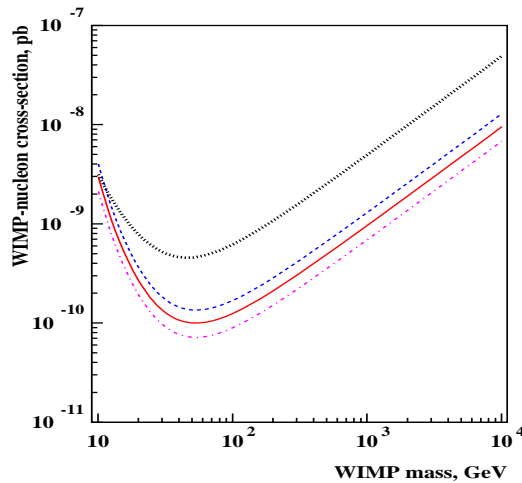

Figure 13: Sensitivity of a future 250 kg xenon detector (one year run time). Dotted line – using 169 2-inch R8778 PMTs surrounded by hydrocarbon shielding. Dashed line – with neutron absorbing light guides and scintillator veto system, background statistically subtracted. Solid line – detector with active veto assuming further improvements in a PMT design (large PMTs with lower contamination levels), background statistically subtracted. Dashed-dotted curve – ultimate limit with no background events observed in one year, reachable with charge readout and ultra-pure materials.

The dotted line in Figure 13 shows the sensitivity of a detector with 169 2-inch

low background R8778 PMTs surrounded by a hydrocarbon passive shielding. The dashed line corresponds to the sensitivity with a scintillator veto system around the detector, neutron absorbing lightguides and all the background statistically subtracted. The solid line shows the limit achievable by a detector with an active veto, lightguides and future new large PMTs with U/Th levels down to 0.5 ppb. Finally, the dashed-dotted curve shows the ultimate limit for a detector with no background events observed during one year of running, reachable with a charge readout technique and ultra-pure components, for instance, less than 0.01 ppb of U/Th in the copper vessel. The above figures can be scaled up to a larger detector. Assuming 0.01 ppb of U and Th in a 350 kg copper vessel is the only source of neutron background and a 250 kg liquid xenon detector has an infinite running time, the nuclear recoil rate in the detector is expected to be 0.2 events per year and the sensitivity to WIMP-nucleon cross-section, which can be achieved with such a rate without background subtraction, is about 6×10^{-12} pb at the minimum of the sensitivity curve.

5   Directional Dark Matter Searches

Most technology for dark matter detectors, such as that adopted for the ZEPLIN experiments of the UKDMC (see sec. 4), focus on obtaining discrimination of nuclear recoils from background electron recoils. However, there remains the possibility that some other systematic or unknown background, such as an unidentified flux of neutrons, may also produce nuclear recoils and that if a signal is seen that it is not of galactic origin. Therefore, it is preferable to look for some characteristic feature of the WIMP signal that identifies it as from the galaxy. Experiments sensitive to the direction of nuclear recoils provide a means to this objective.

5.1   Directional Basics

In the case of a simple isotropic sphere model of the WIMP halo, the WIMP velocity distribution is Maxwellian with a mean speed of 270 kms^{-1}. The closeness of this to the solar velocity (220 kms^{-1} at our orbital radius of 8.5 kpc) means that the velocity distribution of WIMPs in the Earth's rest frame is strongly peaked in the direction of the solar motion. Given the simple kinematical relation between the incoming WIMP direction and the outgoing recoil direction, the distribution

of recoil directions will be strongly anti-correlated with the solar motion direction. Detection of this, via measurement of the directions of nuclear recoils as well as their energies, and hence correlation of the WIMP flux direction with the direction of the solar motion, would provide perhaps the strongest evidence for the existence of WIMPs in our galaxy.

There are two routes to using this directional information in a suitable detector. Firstly, recoil directions measured in the laboratory can be transformed to a direction in galactic coordinates and the distribution of angles between the recoil direction and the direction of solar motion examined for deviations from isotropy. Monte Carlo simulations indicate that as few as 100 identified recoil events are needed to determine a non-isotropic, and hence galactic, recoil signal at >90% confidence.[21] Even a non-isotropic background in the laboratory will appear near isotropic in galactic coordinates due to the Earth's rotation washing out any non-isotropic features. Secondly, the rotation of the Earth means that the average recoil direction in the laboratory frame rotates over 24 sidereal hours, rather than diurnal hours. It is improbable, if not impossible, for any Earth-based background signal to mimic these signatures.

Although there are clear advantages for a detector capable of measuring the directions of nuclear recoils the technology needed represents a considerable challenge. The low energy scale of WIMP induced nuclear recoils (sub-100keV) means that their ranges in solids and liquids are $\sim$100Å, making directional measurement nearly impossible in targets of sufficient mass. Phonon technology, anisotropy in BaF_2 crystals, roton anisotropy in liquid He and organic scintillators such as stilbene have been investigated.[22–25] All of these have encountered problems. An alternative is to use a low pressure gas in a time projection chamber (TPC) so that the recoil range can be extended to a few millimeters. So far this technology, developed by the DRIFT collaboration (comprising the UKDM, Occidental College and Temple University) is the only one that has been developed sufficiently for use in a direction sensitive dark matter experiment. The remaainer of this section describes the DRIFT project and future prospects for directional detection.

5.2   The DRIFT Concept

The DRIFT (Directional Recoil Identification From Tracks) concept uses a time projection chamber (TPC) filled with a negative ion gas at low pressure (typically

40 Torr).[26–28] Track directions can be measured by drifting ionization produced along the recoil track to a suitable readout plane, with the third track dimension being provided by recording the arrival times of charge on the readout plane. Extremely high background rejection is possible in principle via measurements of the track range and because the lower dE/dX of electrons compared with recoils means that the charge deposited per readout element is much lower for electron tracks than for nuclear recoil tracks. The use of negative ions, notably CS_2, to capture and drift the ionization electrons eliminates the need for magnets to reduce diffusion. Underground operation necessary for a dark matter experiment rules out the use of magnets due to size and power requirements. Experiments have shown that the diffusion can be reduced to 0.5mm over drift lengths of 50cm using CS_2.[29,30]

5.3   DRIFT I

The DRIFT I detector is a technology demonstrator experiment built by the collaboration based on the concepts above. It is the first project of the DRIFT programme and the world's first large-scale dark matter detector with potential to measure the direction of WIMP induced nuclear recoils. A picture of DRIFT I under construction is shown in Figure 14.
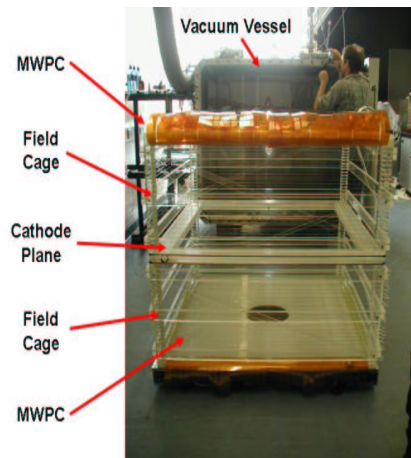

Figure 14: The DRIFT I detector.

Key components of the detector are detailed as follows:

The Containment Vessel: This comprises a $1.5 \times 1.5 \times 1.5$ m vacuum vessel constructed from low background selected 10 mm thick stainless steel with front and back flanges for access and removal of the inner detector. An inner layer of high purity 3 mm copper sheet plus Lucite is used to shield the gas from low energy gammas from the vessel and prevent electrostatic discharges. Quartz windows allow visual inspection. A high voltage feed-through to the central cathode rated at 50 kV is provided through the back flange. Other connections include target gas feeds, slow control feeds and 20 32-way low-background soldered-in DIN connectors for signal lines. Mounted inside, on the roof of the vessel, is a remote controlled ^{55}Fe X-ray source for detector calibration.

The Inner Detector: Inside the vessel is the detector itself, comprising a stand-alone, rectangular and removable drift stack with two back-to-back, horizontal drift volumes each of 0.5 m^3 giving a total detector volume of 1 m^3 (see Figure 15). The two drift volumes are each defined by a 0.5 m^3 high drift field cage, mounted either side of a horizontal, central cathode plane. Readout is provided at either end (top and bottom) by two 1 mm^2 MWPC readout planes. The two field cages use 1 mm thick low background stainless steel wire of 20 mm pitch wrapped on 50 mm Lucite posts with high voltage supplied via a resistor tree with selected resistors mounted on a corner post. The central cathode comprises a 1 m^2 plane of 512 stainless steel wires of diameter 20 μm and pitch of 2 mm. The two MWPC readout planes each consist of an anode plane instrumented with a further 512 20 μm stainless steel wires at a pitch of 2 mm. Orthogonal to this are two grid planes each consisting of 512 100 μm, 2 mm pitch, stainless steel wires at a distance of 10 mm above and below the anode plane.

Voltage Supply and Signal Readout: Power for the central cathode and field cage is supplied via a single vacuum-sealed feed-through and filter circuit. A typical cathode / field-cage input voltage is 20 kV giving a uniform drift field of 250 Vcm^{-1} and a drift velocity for negative ions in 40 Torr of CS$_2$ of 26 ms^{-1}. Power for the upper and lower MWPC units is supplied independently. The MWPCs are typically operated at 3.2 kV giving an ionization multiplication (gain) of $>10^3$ in the grid-anode plane gap. Signals on the 1024 anode wires (512 in each MWPC) are recorded individually using a set of purpose built VME based data acquisition boards with 10^6 samples.s^{-1}, 12-bit waveform digitization, designed and supplied through SLAC. The MWPCs permit a 2D reconstruction of tracks: the horizontal (X axis) extent ΔX being determined by the number of anode wires hit and
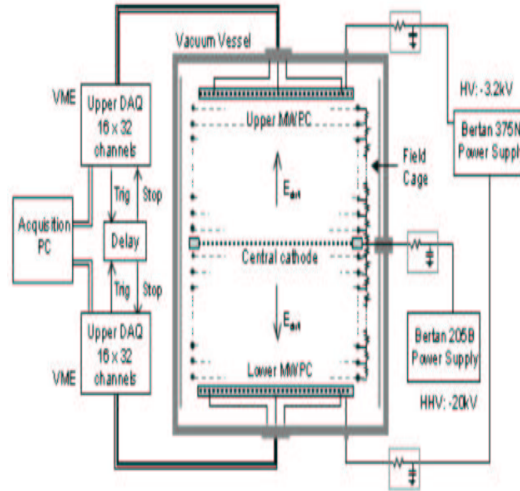
Figure 15: Schematic of the DRIFT I detector.

the vertical (Z axis) extent ΔZ by the pulse width and the relative arrival time of signals. These outputs allow a crude 2D range estimator R2 to be defined as $(R2)^2 = (\Delta X)^2 + (\Delta Z)^2$.[28] The lack of the third (Y) dimension is not expected to significantly reduce the sensitivity of the detector. Simulations also show that background rejection efficiencies of 99.9% are achievable via range/ionization discrimination[26] (see sec. 4). The outer (upper and lower) grid wires are used to provide a veto against alpha particles from the vessel walls or field cage wires incident in the Y direction. Alphas from the X direction can similarly be vetoed by eliminating any event leaving a signal on the edge-most anode wires.

Gas Handling: DRIFT I is operated in continuous gas flow mode to ensure purity. A dry rotary pump is used to draw 99.9% pure CS_2 from a 4 liter canister, through the vessel and out to an output canister. Any waste gas is absorbed by two 75 kg activated charcoal filters. A gas flow controller is used to balance the input CS_2 flow rate (typically about 17 g/hour) with the pump throughput rate, maintaining a constant vacuum vessel pressure.

Safety and System Monitoring: CS_2, although used in low quantities here, requires stringent safety precautions, for instance to prevent leaks. Thus provision is made to monitor key detector parameters via a dedicated slow control PC including: vessel pressure, CS_2 flow rate, laboratory air quality; vessel, DAQ and laboratory temperature, status of high voltages, currents and DAQ noise. An

automatic shut-down sequence is triggered if parameters exceed certain set values, in particular if the vessel gas pressure fluctuates by >2%.

DRIFT-I was installed in the Boulby Underground Laboratory in late 2001. At 1100 m the laboratory is amongst the world's deepest, it has a cosmic ray muon flux of 4.1×10^{-8} cm^{-2} s^{-1} comparable to that at Kamioka and Gran Sasso.[1,2,4] The laboratory provides a clean, air conditioned, dust free environment with facilities including a mechanical workshop, three 2 ton cranes, electrical supply, telephone and Ethernet communications via a 100 Mbit/s optical link to the surface.

First underground testing has been directed at studying stability and response to neutron, gamma and alpha sources. Tests with a collimated ^{241}Am alpha source positioned within the vessel and directed into the top drift volume 25 cm above the central cathode and parallel to it provide a useful means of evaluating the functionality of the detector. Figure 16 shows typical digitized voltage waveforms for an alpha event with trigger threshold set to 200 NIPs (Number of Ion Pairs) together with the reconstructed track length used to determine R2. The NIP value on a given wire is proportional to the energy deposited on that wire and, for a fully contained event, the total NIPs of all triggered wires is proportional to the energy of the event.
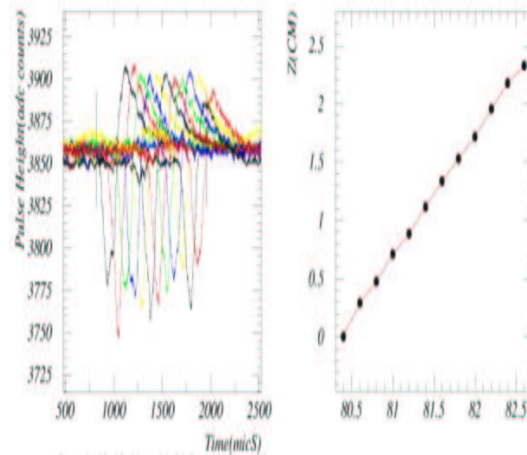

Figure 16: Example alpha event and reconstruction in DRIFT I.

Previous simulations and tests using a prototype 1 ft^3 detector[28,32] have shown that the dE/dX for gammas (electron tracks) is sufficiently low that by careful selection of peak height trigger threshold set on the individual wires it is possible to

reject gammas interacting in the main volume with near 100% efficiency. Results indicated 99.99% rejection above 5 keV for 5% loss of neutron events. This data was used to set the gamma rejection threshold on DRIFT I and neutron tests repeated using a ^{252}Cf source to confirm discrimination. Figure 17 shows results of R2 vs. NIPs obtained for events recorded during this neutron exposure. In spite of the high gamma flux associated with the ^{252}Cf no gammas are seen at high R2, consistent with the rejection efficiency measured with the 1 ft^3 and with Monte Carlos. Based on this result it is estimated that DRIFT I can be operated as an essentially zero gamma background detector with no need for gamma shielding and no need for active R2 gamma rejection analysis. This yields a predicted sensitivity reach around 10^{-6} pb.
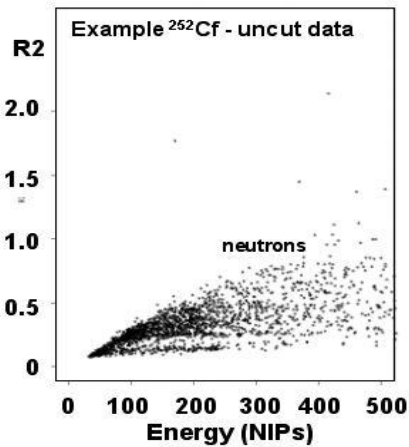

Figure 17: R2 vs. NIPs obtained for events recorded during a typical neutron calibration exposure.

Gamma events interacting directly in the MWPCs produce fast events, because the ionization occurs close to the anode charge multiplication region, that can easily be rejected but nevertheless provide a means, using the internal 5.9 keV ^{55}Fe source, of measuring the detector gain and operational stability. Figure 18 shows two typical distribution of energy deposition values taken about 1 month apart. From the peak position it can be seen that reasonable stability is achieved (<5% drift over 1 month). Further measurements using the source yield a gain of 1500 at the nominal operating voltage of 3.2 kV. At this gain the carbon recoil

energy threshold is 15 keV in full acceptance mode and 25 keV in gamma rejection mode.
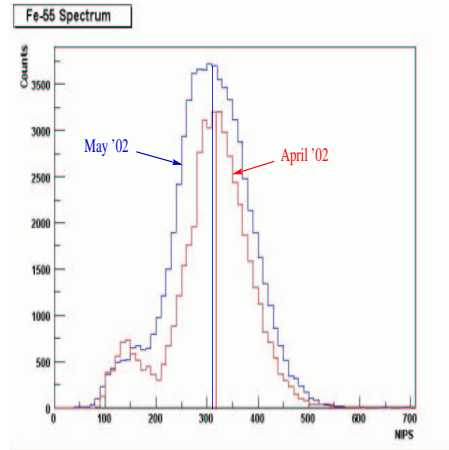

Figure 18: ^{55}Fe spectra from DRIFT I.

5.4   DRIFT II, III and Micromegas Operation

The next phase of DRIFT I will involve assessment of the in-situ directional sensitivity using neutron sources and measurement of the rock neutron background. The detector will then be surrounded by 30 cm of hydrogenous neutron shielding. This is sufficient to reduce the background neutron flux by about 10^3 to yield an interior neutron rate of <1 neutron event per year. With neutron shielding installed DRIFT-I is expected to run for 2 years.

Building on DRIFT I the long term objective of the DRIFT programme is to scale-up detectors towards a target mass of 100 kg (DRIFT III) through development of an intermediate scale module (DRIFT II) that can be replicated many times. A schematic of one DRIFT II module vessel design is shown in Figure 19. This detector has several features designed to improve sensitivity over DRIFT I. In particular grid plane readout is to be incorporated to allow 3D reconstruction of tracks and improved position resolution towards 0.1 mm. Operation at 160 Torr will allow increased target mass per module. A major aim of the programme is to increase the spatial resolution of the sense-plane technology so that pressures can be further increased. Resolution in the direction perpendicular to the MWPC

anode wires is limited to the wire separation which in turn cannot, for mechanical and electrostatic reasons, be reduced to much less than 1 mm. Thus for future DRIFT detectors there is motivation to develop alternative readout technologies capable of position resolutions of 100 mm or less.
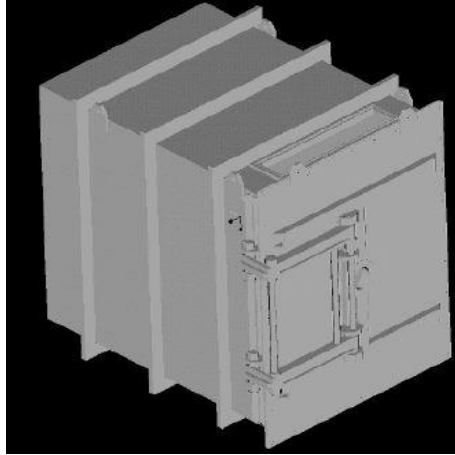

Figure 19: Scematic of one DRIFT II module.

Micromegas[33–35] provides a promising route to this spatial resolution increase. Micromegas is essentially a scaled-down parallel-plate avalanche chamber consisting of a thin, perforated nickel or copper foil maintained at a constant distance above an anode plane by insulating pillars. It has several characteristics that make it suitable for next-generation DRIFT detectors: simplicity and ease of construction; resistance to spark damage; low activity materials (Kapton, copper); high energy resolution; flexibility of readout geometry; large areas possible (50 x 50 cm has been demonstrated[36]).

To investigate the suitability of Micromegas for operation with negative ion drift, apparatus was constructed comprising a 45 mm diameter Micromegas with single-anode readout mounted inside a 20 cm diameter vacuum vessel. The cathode was constructed from woven stainless steel cloth (52.9% open area) stretched on an insulating frame, defining a drift region of 17.5 mm. The active area was defined by the copper micromesh, supported on a 2 mm PCB frame clamped to the anode. Signals were passed to a Canberra 2003BT preamplifier and then to a Tennelec TC243 shaping amplifier with gain set to ×50 and a shaping time of 0.5 ms. The unipolar output was passed to a Tennelec multichannel analyzer.

This was linked via GPIB interface to a computer running Oxford PCA-Multiport software for recording energy spectra. Figure 20 shows preliminary results of the ^{55}Fe energy spectrum obtained from CS_2 at 230 Torr. The energy resolution in this case is 16.9% and the gain, based on a W-value in CS_2 of 19.7 per ion pair, is $520 +/- 70$.
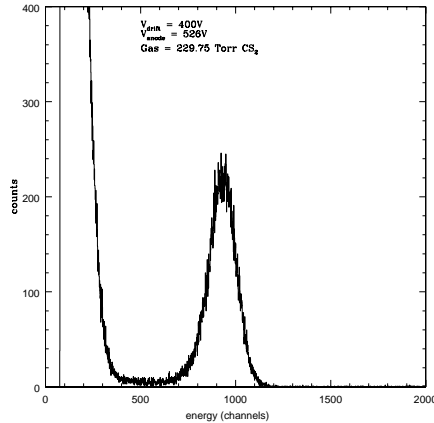

Figure 20: ^{55}Fe spectrum from the Micromegas test detector operated with CS_2.

6   Conclusion

Liquid xenon has been demonstrated as an excellent technology for dark matter searches with ZEPLIN I already producing significant sensitivity using single phase pulse shape discrimination. The UKDM and collaborators are now progressing to two phase operation which shows promise for substantial improvement in sensitivity towards 10^{-8} pb. Perhaps more significantly there is a route with this technology to reach towards 10^{-10} pb with a 1 tonne liquid xenon detector. We have shown that the neutron background from rock, muon and detector neutrons can in principle be suppressed sufficiently to reach this goal.

Directional detectors based on low pressure gas provide a unique means of determining the galactic origin of an observed WIMP signal, a significant advantage over conventional dark matter experiments. The DRIFT programme based on this concept is underway to approach this possibility, complementing also the liquid xenon programme through use of entirely different technology with target

nuclei of lower atomic weight. DRIFT I is currently producing first engineering data underground while scale-up detectors DRIFT II and III are under development. Micromegas has been demonstrated to work with CS_2 and therefore offers a possible route to increasing the spatial resolution of DRIFT-type directional detectors and hence the target pressure. This is desirable as a means of reducing the volume of detector modules required for a large scale DRIFT detector.

References

[1] S.M. Paling et al. (UK Dark Matter Collaboration), *Proc. 4th International Workshop on the Identification of Dark Matter*, York UK, World Scientific (2002) 440; contact the author for further details.

[2] V. A. Kudryavtsev, N. J. C. Spooner and J. E. McMillan. *Nuclear Instrum. & Meth. in Phys. Res. A*, **505** 688 (2003).

[3] M. Robinson et al. *Nuclear Instrum. & Meth. in Phys. Res. A*, **511** 347 (2003).

[4] P. F. Smith et al. (UK Dark Matter Collaboration) *Phys. Lett. B* **379** 299 (1996).

[5] B. Ahmed et al. (UK Dark Matter Collaboration) *Astroparticle Physics* **19** 691 (2003).

[6] R. Bernabei et al. *Nucl. Phys. A* **719** 257 (2003).

[7] D. Abrams et al. *Phys. Rev. D* **66** 122003 (2002).

[8] A. Benoit et al. *Phys. Lett. B* **13** 15 (2001).

[9] P. Benetti et al. *Nucl. Instrum. & Meth. in Phys. Res. A* **327** 203 (1993).

[10] P. Benetti et al. *Nucl. Instrum. & Meth. in Phys. Res. A* **329** 361 (1993).

[11] M.J. Carson et al. submitted to *Astroparticle Physics* (2003).

[12] S. Agostinelli et al. *Nucl. Instrum. & Meth. in Phys. Res. A* **506** (2003) 250; see also the GEANT4 web-page at CERN: `http://geant4.web.cern.ch/geant4`.

[13] A. Fassò, A. Ferrari and P. R. Sala. *Proceedings of the MonteCarlo 2000 Conference* (Lisbon, October 23-26, 2000), Ed. A.Kling, F.Barao, M.Nakagawa,

L.Tavora, P.Vaz (Springer-Verlag, Berlin, 2001), p. 159; A. Fassò, A. Ferrari, J. Ranft and P. R. Sala, *ibid.* p. 995.

[14] R. M. McAlpine. Electron Tubes Ltd. Private communications, see also `http://www.electron-tubes.co.uk/`.

[15] Hamamatsu Photonics KK Ltd., private communication; see also talk by M. Nakahata for the XMASS Collaboration at LowNu2003 Workshop, `http://cdfinfo.in2p3.fr/LowNu2003/`.

[16] F. Sauli et al. *Nucl. Instrum. & Meth. in Phys. Res. A* **386** (1997) 531.

[17] Y. Giomataris et al. *Nucl. Instrum. & Meth. in Phys. Res. A* **376** (1996) 29.

[18] A. Buzulutskov et al. Submitted to *IEEE Trans. on Nucl. Sci.* physics/0308010.

[19] B. Morgan et al. (for the DRIFT and UK Dark Matter Collaborations). *Nucl. Instrum. & Meth. in Phys. Res. A*, in press.

[20] J. D. Lewin and P. F. Smith. *Astroparticle Physics* **6** (1996) 87.

[21] M.J. Lehner et al. *Proc. 2nd International Conference on Dark Matter in Astro and Particle Physics*, Heidelberg, Inst. of Physics, 767 (1998).

[22] R.J. Gaitskell et al. *Nucl. Instrum. & Meth. in Phys. Res. A* **370** 162 (1996).

[23] J.S. Adams et al. *Phys. Lett. B* **341** 431 (1995).

[24] N.J.C. Spooner et al. *Proc. 1st International Workshop on the Identification of Dark Matter*, Sheffield UK (1996), World Scientific, 481 (1996).

[25] P. Belli et al. *Nuovo Cimento C* **15** 475 (1992).

[26] D.P. Snowden-Ifft et al. *Phys. Rev. D* **61** 1 (2000).

[27] B. Lawson. *PhD Thesis*, University of Sheffield, (2002).

[28] D.P. Snowden-Ifft et al. *Nucl. Instrum. & Meth. in Phys. Res. A* **498** 155 (2003).

[29] C.J. Martoff et al. *Nucl. Instrum. & Meth. in Phys. Res. A* **440** 355 (2000).

[30] T. Ohnuki et al. *Nucl. Instrum. & Meth. in Phys. Res. A* **46** 142 (2001).

[31] V.A. Kudryavtsev et al. *Proc. 4th International Workshop on the Identification of Dark Matter*, York UK, World Scientific 477 (2002).

[32] T.B. Lawson et al. *Proc. 4th International Workshop on the Identification of Dark Matter*, York UK, World Scientific 338 (2002).

[33] Y. Giomataris et al. *Nucl. Instrum. & Meth. in Phys. Res. A* **376** 29 (1996).

[34] Y. Giomataris et al. *Nucl. Instrum. & Meth. in Phys. Res. A* **419** 239 (1998).

[35] A. Delbart et al. *New Developments of Micromegas Detectors* DAPNIA-SED-01 (2000).

[36] J.P. Cussonneau et al. *An Integration of Micromegas based Muon Tracking Chambers in Alice*, `http://documents.cern.ch/archive/electronic/cern/others/ALI/Note/INT-1998-54.pdf`.